

Surface Structure on Ar⁺-Ion Irradiated Graphite by Scanning Probe Microscopy

Bai AN¹, Seiji FUKUYAMA¹, Kiyoshi YOKOGAWA^{1,*} and Masamichi YOSHIMURA²

¹Chugoku National Industrial Research Institute, AIST, MITI, Kure, Hiroshima 737-0197, Japan

²Toyota Technological Institute, Hisakata, Tempaku, Nagoya 468-8511, Japan

(Received January 17, 2000; accepted for publication March 23, 2000)

The surface structure of a highly oriented pyrolytic graphite (HOPG), irradiated by Ar⁺ ions with an ion energy of 0.5–1.0 keV at doses below 5×10^{11} ions/cm² during annealing, was characterized by scanning probe microscopy. The ion-induced hillocks were observed by both scanning tunneling microscopy (STM) and atomic force microscopy (AFM) after the ion irradiation, the heights of which, measured by STM, were larger than that measured by AFM in the tapping mode. The hillocks were recovered distinguishably by annealing above 470 K. Almost 85% of the hillocks disappeared after annealing at 1270 K and they disappeared completely after annealing above 1770 K. The behavior of defects produced by ion-irradiation in HOPG during annealing is discussed.

KEYWORDS: STM, AFM, surface structure, ion bombardment, graphite, annealing

1. Introduction

Ion implantation techniques have been widely applied in micro- and nano-technologies, and ion-irradiation induced defects on an atomic scale on solid surface have been investigated by scanning probe microscopy (SPM).^{1–8)} The surface structures produced by various levels of energy and various kinds of ions on highly oriented pyrolytic graphite (HOPG) were studied by scanning tunneling microscopy (STM), and it was observed that irradiation using energetic ions such as argon, neon and krypton above 100 eV, generally produced small protrusions, called hillocks, with diameters of a few nm and heights of several angstroms.^{1–8)} Atomic force microscopy (AFM) has been used to characterize the surface structure of ion-irradiated HOPG together with STM.^{7,8)} Mochiji *et al.*⁷⁾ carried out ion-irradiation on HOPG with highly charged Ar ions of Ar⁺, Ar⁴⁺ and Ar⁸⁺ at 2–15 keV and doses below 10^{13} ions/cm², and they did not observe any surface irregularities by AFM in the contact mode. Ogiso *et al.*⁸⁾ also carried out ion-irradiation on HOPG with Au ions at 3.1 MeV and doses of 1.9×10^{11} ions/cm², and they observed a reverse contrast image by changing the friction force between the tip and the specimen by UHV-AFM in the contact mode, and they did not observe surface irregularities by AFM in the non-contact mode. These results indicated that the hillocks with lattice damage observed by STM do not always correspond to those by AFM.

Despite the above mentioned previous studies,^{1–8)} the topographical structure of the surface damage on graphite, produced by energetic ion impact above 100 eV, has not been determined yet. Even though the recovery processes of the damage at atomic scale induced by ion-irradiation in graphite are important to control defects, few SPM studies have been conducted on this aspect. In this study, we investigated the surface structure of HOPG irradiated by Ar⁺ ions with an ion energy of 0.5–1.0 keV at doses below 5×10^{11} ions/cm² during annealing, by STM and AFM in the contact and the tapping modes. The topographical structure of the ion-induced damage on HOPG and the recovery processes of the damage were discussed.

2. Experimental

The HOPG specimen was cleaved in air and irradi-

ated by Ar⁺ ions with ion energies of 0.5–1.0 keV in an ultra-high vacuum (UHV)-STM chamber. Doses below 5×10^{11} ions/cm² were used to avoid overlapping of cascades.¹⁾ The ion-irradiated specimen was resistively annealed in vacuum below 10^{-6} Pa at elevated temperatures up to 1873 K for 10 min. The temperature of the specimen was measured using an optical pyrometer outside the chamber. The temperature below 873 K was estimated from the plot of the temperature versus the square of the electronic current. STM observations were performed in both UHV and ambient atmosphere using commercially available Pt/Ir tips, in the constant current mode with a tip bias of 100–500 mV and a tunneling current of 0.5–1.5 nA. AFM observations in the contact and tapping modes were performed in ambient atmosphere using a commercially available silicon nitride cantilever and a silicon cantilever, respectively.

3. Results

Typical STM and AFM images obtained on the HOPG surface as-irradiated by Ar⁺ ions at 1.0 keV are shown in Fig. 1. Small discrete hillocks with diameters of 1–3 nm and heights of 0.2–0.8 nm are observed on the surface by STM as shown in Fig. 1(a). The hillocks are seen as bright images with a disordered structure in the triangular structure of graphite on the surface, and a spot-like superstructure of $(\sqrt{3} \times \sqrt{3})R30^\circ$ of graphite is observed close to them, as shown in the inset of Fig. 1(a). This STM image is similar to those obtained in previous studies.^{1–8)} The hillocks with heights of 0.08–0.15 nm can be observed at the Ar⁺-irradiated regions by AFM in the tapping mode independent of scanning direction as shown in Fig. 1(b), while reverse contrast image by the change in the friction force between the tip and specimen is observed on the Ar⁺-irradiated regions by AFM in the contact mode (not shown here), as reported by Ogiso *et al.*⁸⁾ The number of hillocks identified by AFM in the tapping mode in (b) is as many as those identified by STM in (a). The heights of the ion-induced hillocks measured by STM are larger than those by AFM in the tapping mode. Similar results were also obtained on the surface irradiated by Ar⁺ ions at 500 eV.

These ion-induced hillocks are recovered rapidly by annealing above 470 K. The STM images obtained on the surfaces annealed at 830 and 1270 K are shown in Fig. 2. Many of the ion-induced hillocks distinctly disappear at 830 K as shown in Fig. 2(a) in comparison with those prior to annealing as shown in Fig. 1, and a few hillocks still appear after

*Corresponding author. E-mail address: kyokoga@cniiri.go.jp

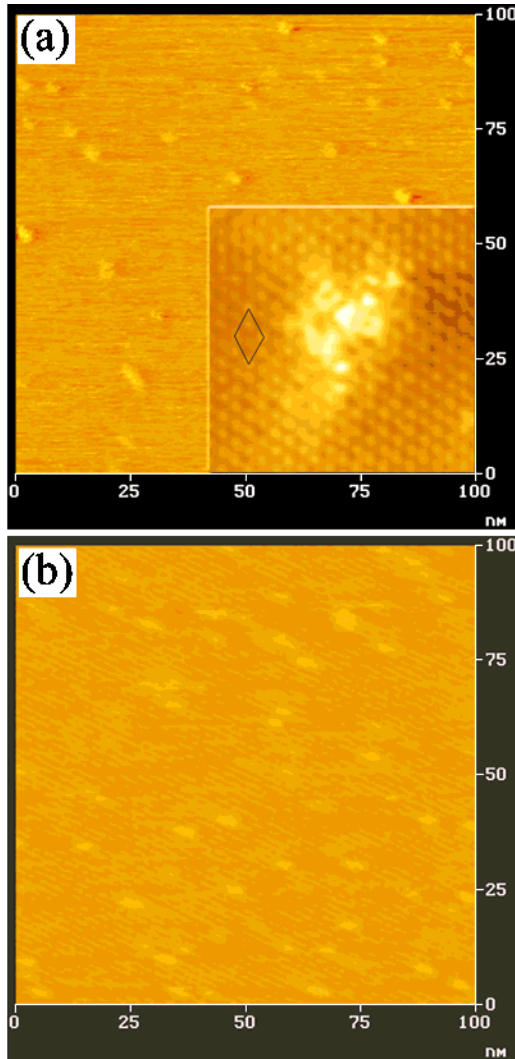


Fig. 1. STM image (a) and AFM image in the tapping mode (b) on HOPG as-irradiated by Ar⁺ ions at 1.0 keV. (A rhombus shows a unit cell of the spot-like superstructure of $(\sqrt{3} \times \sqrt{3})R30^\circ$ of graphite in the inset of (a).)

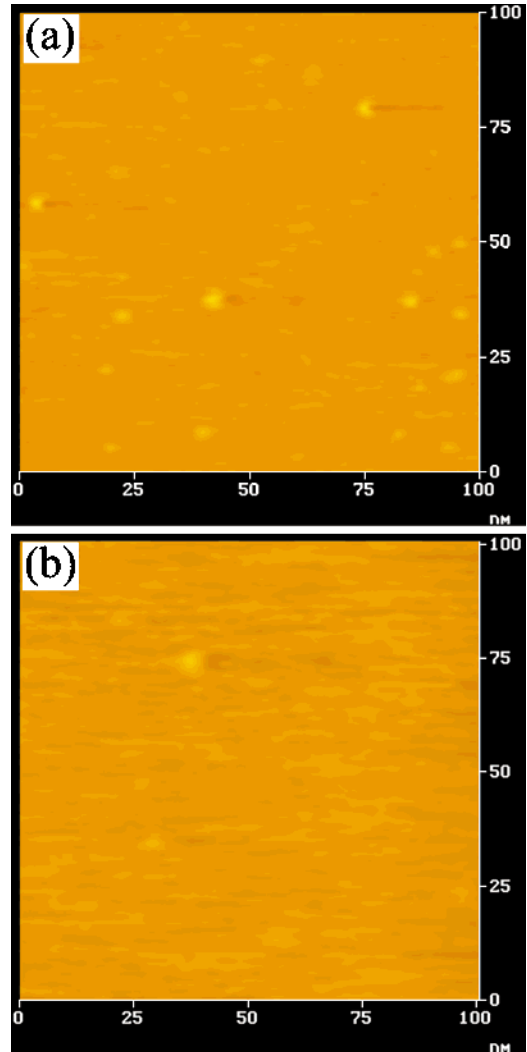


Fig. 2. STM images on HOPG irradiated by Ar⁺ ions at 1.0 keV after annealing at 830 K (a) and 1270 K (b).

annealing at 1270 K in Fig. 2(b). The effects of annealing temperature on the density of hillocks induced by Ar⁺ ions with 1.0 keV is shown in Fig. 3. The density of the hillocks is analyzed from more than twenty STM images in a unit scan area of $100 \times 100 \text{ nm}^2$ obtained from different areas of each specimen. The density of hillocks rapidly decreases above 470 K. Almost 85% of the hillocks disappear at 1270 K and they completely disappear above 1770 K.

Two types of defects at atomic resolution, one is the protrusion having undisturbed lateral atomic arrangement of graphite and another is the multiple vacancy, were observed on the Ar⁺ ion-irradiated surface after annealing above 830 K. Figure 4 shows a typical STM image of these two types of defects after annealing at 1270 K. The STM image of the protrusion type defect with undisturbed lateral atomic arrangement of graphite is shown in Fig. 4(a). The cross section of the defect along the line ab in the image is shown in Fig. 4(b). It is observed that a few tens of atoms at the center of the image gradually protrude from the undisturbed atoms surrounding the center. The height of the protrusion measured at the cross section is around 0.1 nm. The STM image of the multiple-vacancy-type defects is shown in Fig. 4(c). A dark

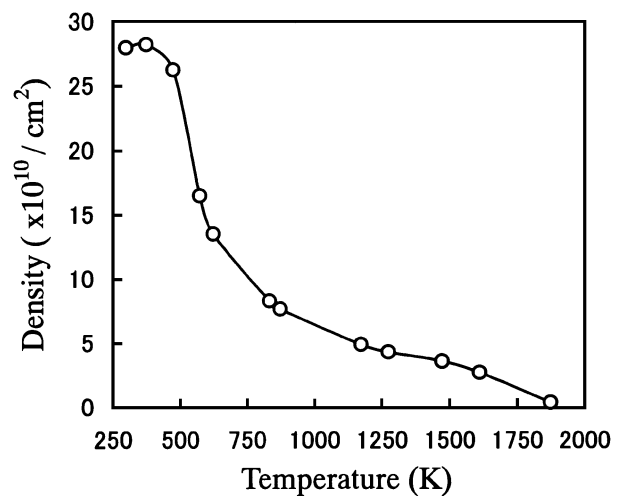


Fig. 3. Effects of annealing temperature on the density of hillocks induced by Ar⁺ ions at 1.0 keV on HOPG.

spot is observed at the center of the image, close to which the spot-like superstructure of $(\sqrt{3} \times \sqrt{3})R30^\circ$ of graphite is observed within a diameter of 4 nm, but no symmetric image is observed around the dark spot. The cross section of

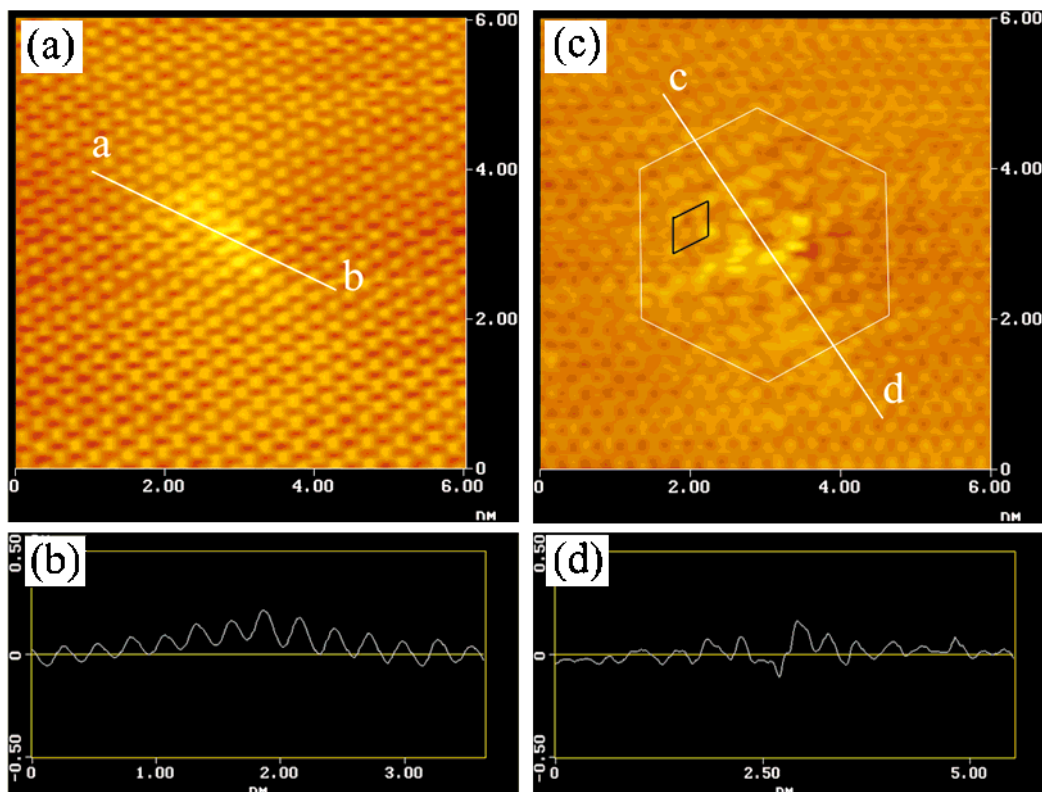


Fig. 4. STM images of the protrusion type and the multiple-vacancy-type defects on HOPG irradiated by Ar^+ ions at 1.0 keV at atomic resolution after annealing at 1270 K. ((a): a protrusion-type defect, (b): cross section along the line ab in (a), (c): a multiple-vacancy-type defect, (d): cross section of the line cd in (c)) (A rhombus shows a unit cell of the spot-like superstructure of $(\sqrt{3} \times \sqrt{3})R30^\circ$ of graphite in (c).)

the defect along the line cd in the image indicates that the dark spot is a hollow defect as shown in Fig. 4(d). Mizes and Foster⁹⁾ performed simulations on the electronic perturbation caused by single point and multiple point defects. They showed that a single point defect results in a superlattice and forms a three-fold symmetry around the defect, while a multiple point defect leads to the loss of the three-fold symmetry. Kondo *et al.*¹⁰⁾ and Kelly *et al.*¹¹⁾ experimentally observed the electronic perturbation with three-fold symmetry caused by a single point defect. It is identified that the defect shown in Fig. 4(c) is a multiple-vacancy type. These two types of defects disappeared from the surface of the specimen after annealing above 1770 K.

4. Discussion

It is well known that incident Ar^+ ions initiate collision cascades in HOPG, resulting in interstitials and vacancy-type defects along the ion track. Studies on ion-irradiation of graphite have been conducted by transmission electron microscopy generally before SPM.^{12–14)} It was suggested that a single interstitial could migrate to form clusters of 2–4 carbon atoms between the layers near the surface at room temperature.^{12–14)} It has also been demonstrated by molecular dynamics simulations that interlayer dimers and trimers produce hillocks on graphite with atomic heights of 0.07 and 0.1 nm, respectively.¹⁵⁾ As is well-known, an STM image illustrates the partial electron density near the Fermi energy,¹⁶⁾ while an AFM image in the tapping mode illustrates the total electron density or surface topography without frictional effect¹⁷⁾ which affects the AFM image in the contact mode. We ob-

served topographical hillocks with heights of 0.2–0.8 nm by STM (Fig. 1(a)) and with heights of 0.08–0.15 nm by AFM in the tapping mode (Fig. 1(b)), although Mochiji *et al.*⁷⁾ and Ogiso *et al.*⁸⁾ did not find surface irregularities by AFM. Mochiji *et al.*⁷⁾ used highly charged Ar ions (Ar^+ , Ar^{4+} , Ar^{8+}) at 2–15 keV and Ogiso *et al.*⁸⁾ used Au ions at 3.1 MeV. It is possible that results by AFM depend on the conditions of ion-irradiation. The height of the hillocks measured by AFM in the tapping mode is the same as that obtained by molecular dynamics simulations¹⁵⁾ but is lower than that obtained by STM. Hence, it is considered that the anomalous height of the hillocks obtained by STM as shown in Fig. 1(a) is due to the increase in the partial charge density of states caused by the lattice damage as reported by Mochiji *et al.*⁷⁾ and Ogiso *et al.*⁸⁾

The interstitial atoms and the small interstitial clusters could migrate to recombine with the vacancies or aggregate to form larger clusters of interstitials during annealing above 373 K, while the vacancies could not migrate below 1273 K, hence they could not form larger clusters of vacancy or vacancy loops below 1273 K.^{12–14)} It is considered that the decrease in the number of ion-induced hillocks shown in Figs. 2 and 3 is due to the recombination of mobile interstitials and immobile vacancies. The behavior of defects produced by ion-irradiation during annealing is illustrated in the cross section of HOPG in Fig. 5. The interstitials and vacancies are produced by ion-irradiation as shown in Fig. 5(a). The mobile interstitials move and recombine with immobile vacancies during annealing as shown in Fig. 5(b).

As a result of the recombination of mobile interstitials and

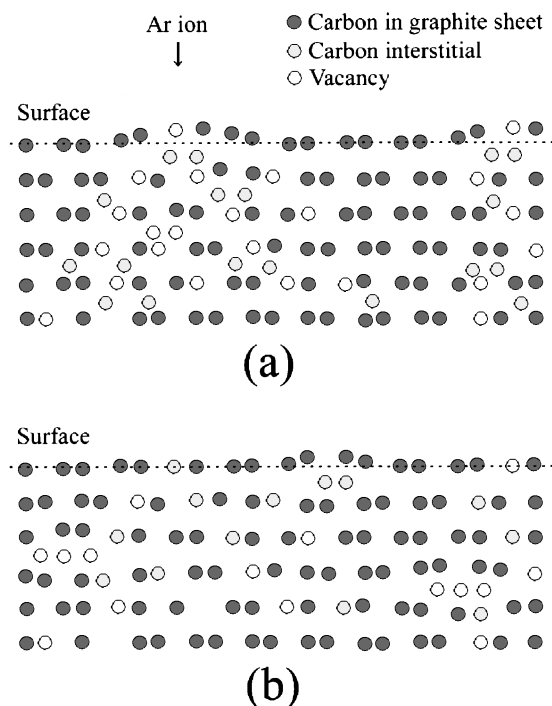


Fig. 5. Illustration of the behavior of the defects produced by ion-irradiation during annealing in the cross section of HOPG. ((a): as ion-irradiated, (b): during annealing)

the immobile vacancies during annealing, the remaining interstitials and vacancies are still observed on the surface after annealing at 1270 K (Fig. 4) as protrusions having undisturbed lateral atomic arrangement of graphite in (a) and multiple vacancy in (c), respectively. It is considered that these remaining defects disappear during further annealing up to 1770 K by rapid diffusion of carbon atoms on the surface, including the recombination of mobile interstitials and mobile vacancies.

5. Conclusions

The surface structure of HOPG irradiated by Ar^+ ions with ion energies of 0.5–1.0 keV at doses below 5×10^{11} ions/cm²

during annealing was characterized by STM and AFM in the contact and tapping modes. The ion-induced hillocks were observed by both STM and AFM after ion irradiation, the heights of which, measured by STM, was larger than that measured by AFM in the tapping mode. It is considered that the interstitials and interstitial clusters created by collision cascade produces the ion-induced topographical hillocks, and the distinct height of protrusions in the STM image is due to the electronic states of the damaged graphite lattice. The hillocks were recovered distinguishably by annealing above 470 K. Almost 85% of hillocks disappeared after annealing at 1270 K and they disappeared completely after annealing above 1770 K due to the recombination of interstitials and vacancies.

- 1) L. Porte, M. Phaner, C. H. De Villeneuve, N. Moncoffre and J. Tousset: Nucl. Instrum. Methods B **44** (1989) 116.
- 2) L. Porte, C. H. De Villeneuve and M. Phaner: J. Vac. Sci. & Technol. B **9** (1991) 1064.
- 3) R. Coratger, A. Claverie, A. Chahboun, V. Landry, F. Ajustron and J. Beauvillain: Surf. Sci. **262** (1992) 208.
- 4) K. P. Reimann, W. Bolse, U. Geyer and K. P. Lieb: Europhys. Lett. **30** (1995) 463.
- 5) W. Bolse, K. Reimann, U. Geyer and K. P. Lieb: Nucl. Instrum. Methods B **118** (1996) 488.
- 6) S. G. Hall, M. B. Nielsen and R. E. Palmer: J. Appl. Phys. **83** (1998) 733.
- 7) K. Mochiji, S. Yamamoto, H. Shimizu, S. Ohtani, T. Seguchi and N. Kobayashi: J. Appl. Phys. **82** (1997) 6037.
- 8) H. Ogiso, W. Mizutani, S. Nakano, H. Tokumoto and K. Yamamoto: Appl. Phys. A **66** (1998) S1155.
- 9) H. A. Mizes and J. S. Foster: Science **244** (1989) 559.
- 10) S. Kondo, M. Lutwyche and Y. Wada: Jpn. J. Appl. Phys. **33** (1994) L1342.
- 11) K. F. Kelly, D. Sarkar, G. D. Hale, S. J. Oldenburg and N. J. Halas: Science **273** (1996) 1371.
- 12) C. Baker and A. Kelly: Philos. Magn. **11** (1965) 729.
- 13) P. A. Throver: Philos. Magn. **18** (1968) 697.
- 14) P. A. Platonov, E. I. Trofimchuk, O. K. Chugunov, V. I. Karpukhin, Yu. P. Tumanov and S. I. Alexeev: Rad. Eff. **25** (1975) 105.
- 15) K. Nordlund, J. Keinonen and T. Mattila: Phys. Rev. Lett. **77** (1996) 699.
- 16) J. Tersoff: Phys. Rev. Lett. **57** (1986) 440.
- 17) G. J. Simpson, D. L. Sedin and K. L. Rowlen: Langmuir **15** (1999) 1429.